Finite Element Modeling and Further Analyses of Deflection and Coating Stress in Coated Cantilever Beams

A PROJECT
SUBMITTED TO THE FACULTY OF THE GRADUATE SCHOOL
OF THE UNIVERSITY OF MINNESOTA
BY

Robert Shurig

IN PARTIAL FULFILLMENT OF THE REQUIREMENTS
FOR THE DEGREE OF
MASTER OF MATERIAL SCIENCE AND ENGINEERING

Lorraine F. Francis, Advisor

January 2011

Acknowledgements

I would like to thank my advisor, Professor Lorraine F. Francis, for her insight, guidance, and patience throughout the process of my research.

I would like to thank Karan Jindal, Christine Cardinal, and Kathleen Crawford for their willingness to share their knowledge of coatings, the stress measurement system, and general laboratory techniques.

I would like to thank Nancy Rowe, David Porter, and Ravi Chityala at the University of Minnesota Supercomputing Institute for their help and guidance toward maintaining my access to the ANSYS software and the management of my data.

Dedication

This project is dedicated to my parents, teachers, coaches, professors, and managers who have invested in me far beyond what was required of them. You have my deepest gratitude.

This project is also dedicated to my sons Garrett and Adam. Your futures are bright.

Table of Contents

List of Tables

List of Figures

1 Introduction

One way to monitor stress development in a coating as it dries and/or cures is to measure the deflection of the substrate under the coating. The substrate often takes the form of a cantilever which is anchored on one end, coated with a liquid, and then deflected as stress evolves in the coating. Deflection of the cantilever is monitored using a laser and a position sensitive photodiode. Relationships based on plate theory, developed by Corcoran [1] and discussed in Appendix A, allow coating stress to be calculated using the known material properties of the cantilever and its observed deflection.

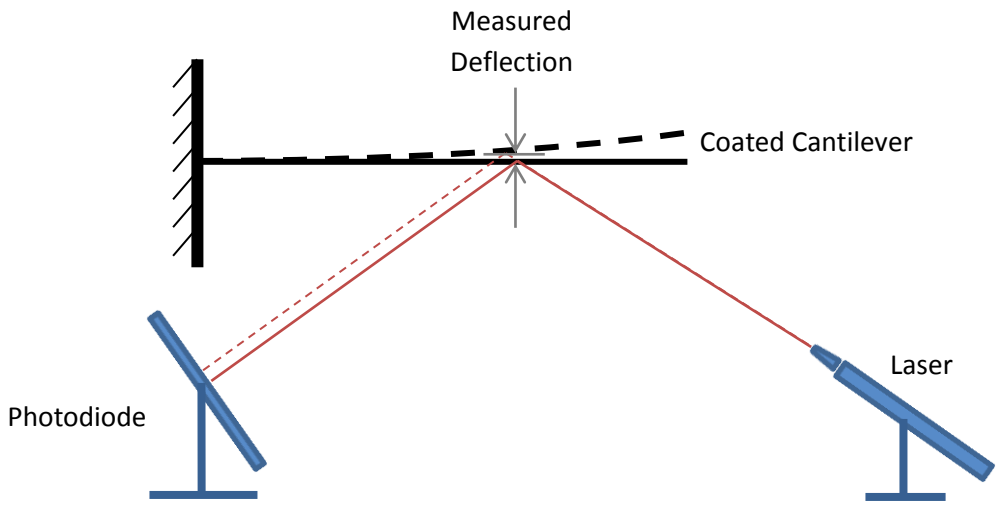

Figure 1: Schematic of an experiment used to calculate coating stress through measurement of cantilever deflection (dashed line indicates deflected cantilever)

Several issues arise from using this coating stress measurement method. One of these is the potential for error introduced to the measurement method if the laser beam is not centered at the midline of the cantilever. Section 2 describes a finite element (FE) analysis which was used to understand the magnitude of this potential error.

Another issue typically encountered with this measurement method is the presence of a drying front that begins at the edges of the cantilever and progresses toward the center until the entire coating has dried. Such fronts create stress gradients within the coating and invalidate the plate theory relationships. It has been found that the application of particular border materials around the edges of the cantilever eliminates this drying front and allows the coating to dry uniformly. FE analysis was used to assess the amount of error introduced to the measurement method by the presence of the border – caused by increased cantilever stiffness as well as incomplete coating coverage where the border overlaps along the edges of the cantilever. These FE analyses, performed on two separate border materials, are described in Sections 3 and 4.

Another FE model was created in order to understand coating stresses under lateral drying conditions. In this model, the lateral drying front was progressed from the outside to the center of the cantilever in a series of steps. This analysis, described in Section 5, shows that the average coating stress increases nearly proportionally with the area behind the drying front. This result suggests that local coating stress in areas behind the drying front could be estimated, despite the presence of a lateral drying

front, by observing the deflection of the cantilever and assigning all of the calculated stress to the dried coating.

Using similar concepts, a method is proposed for deducing the stress contained in a local region of coating, as a function of time, based on the experimental observations of a laterally drying cantilever sample. Sections 6 and 7 describe this method as well as the challenges encountered when the method was applied to an experimental lab sample.

2 Bending along the Cantilever's Short Axis and its Potential Effect on Stress Prediction

2.1 Background

As discussed above, coating stress caused by the drying process results in deflection along the length of the cantilever. This deflection, as measured by the laser beam and sensor, is used to calculate average coating stress in the sample. However, as the coating dries over the cantilever it would also be expected that bending occurs along its short axis as well. This behavior is referred to as "cupping". Because the in-plane stress equations developed from plate theory assume deflection is taken exactly from the mid-line of the cantilever, measurements taken away from the center of the cantilever could appear artificially high due to the additional short-axis deflection caused by cupping. A finite element model was developed and analyzed in order to examine the significance of this potential error.

2.2 Finite Element Model

The model was intended to simulate a coating of ceramic particles (typically alumina or silica) dispersed in water with or without a polymer binder (typically polyvinyl alcohol) over a silicon cantilever and was performed using ANSYS version 12.1 software. Cantilever and coating geometries were based on typical test sample dimensions as follows:

- Cantilever Length = 45 mm
- Cantilever Width = 7 mm
- Cantilever Thickness = 0.400 mm (400 μm)
- Coating Thickness = 0.020 mm (20 μm)

Adjacent volumes representing the cantilever and the coating were joined using the "glue" Boolean operation within ANSYS. A three-dimensional, 20-node structural solid named "Solid95" was chosen as the element type (see Figure 2 below).

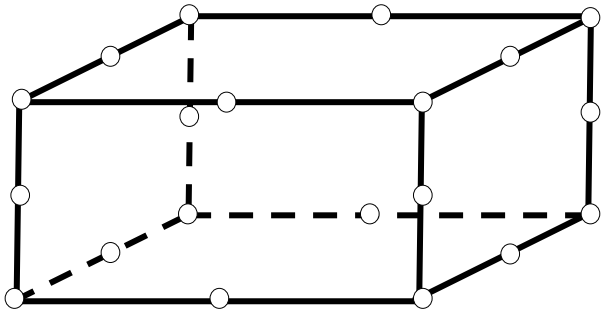

Figure 2: Representation of the "Solid95" 3-dimensional 20-node Structural Solid Element (element boundaries indicated by lines, nodes indicated by open circles)

Material properties were assigned to simulate the silicon cantilever and to estimate the properties of the coating:

- $E_{cantilever}$ = 172 GPa
- $\nu_{cantilever}$ = 0.25
- $E_{coating}$ = 5 GPa
- $\nu_{coating}$ = 0.33

A hexahedral mesh was created by dividing the cantilever into elements of size 0.10 mm x 0.10 mm x 0.10 mm (length x width x height) and the coating into elements of size 0.10 mm x 0.10 mm x 0.02 mm. The model's meshed volumes are illustrated in Figure 3.

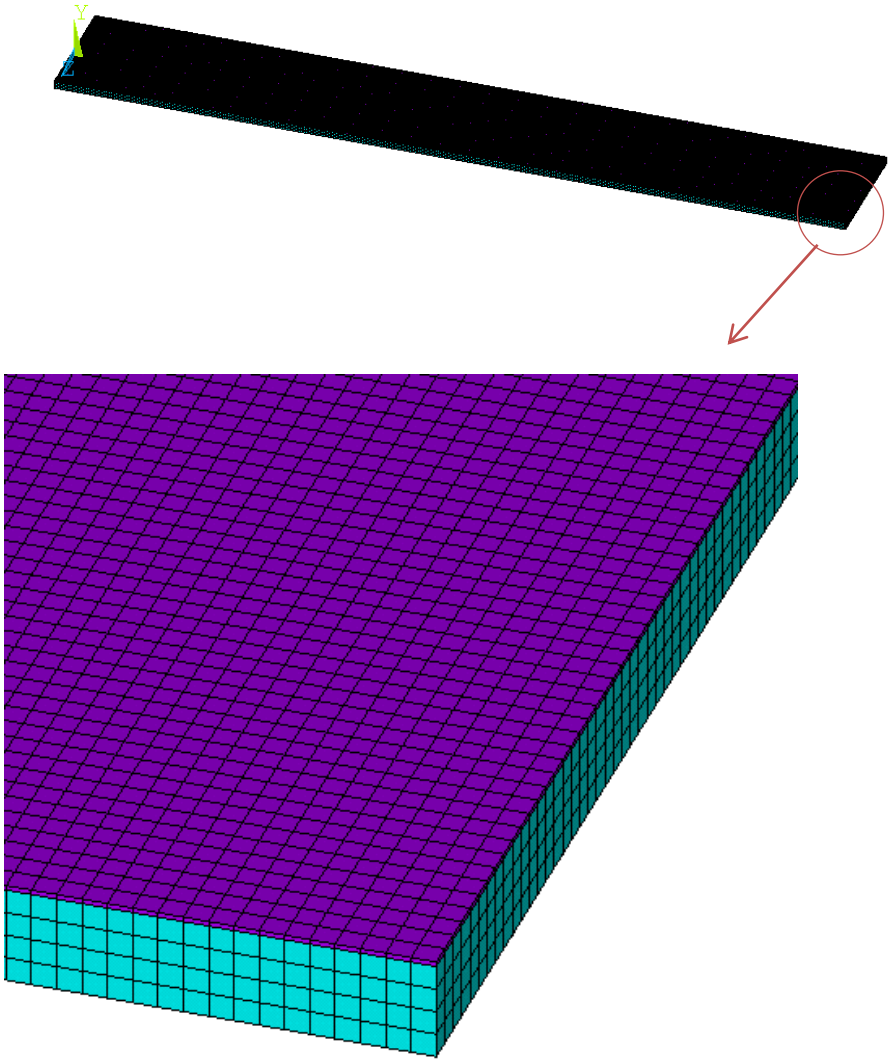

Figure 3: Meshed Volumes of the Cantilever and Coating Model

Coating stress results from constrained shrinkage which develops during the drying process. This constrained shrinkage was replicated in the FE model by applying a thermal contraction to the coating while leaving the cantilever without an applied thermal stress. All coating elements were given a coefficient of thermal expansion of 0.001 [1/degree]. A temperature load of -2 degrees was applied to the

coating resulting in a constrained shrinkage of 0.2%. In order to simulate clamping of the sample into the test apparatus, the cantilever and coating were constrained by setting all degrees of freedom for each area at X = 0 to zero.

2.3 Results and Discussion

The model calculated von Mises equivalent stress of 14.8 MPa throughout most of the coating (i.e. away from the edges). As expected, the solution stress plot, given in Figure 4, shows the cantilever deflecting smoothly upward.

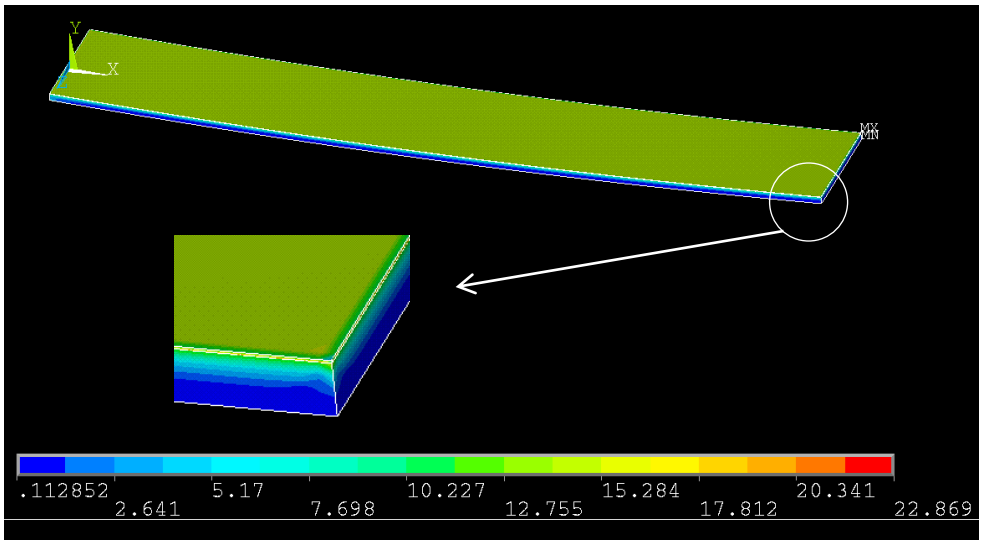

Figure 4: von Mises Equivalent Stress Plot of the Deformed Cantilever and Coating

Deflections for the modeled cantilever were taken from points on the under-side of the cantilever at 30 mm from its clamped/constrained end (X = 30 mm). This represents a typical measurement location targeted by the laser used to detect deflection of lab samples. The model's resulting deflection at this location was 23.74

μm. Using this deflection and the material properties described above, the in-plane stress equations predict an average coating stress of 15.4 MPa (reference Equation A.18 in Appendix A). The von Mises equivalent stress calculated by the model (14.8 MPa) is within 3.6% of the value predicted by the modeled deflection and the in-plane stress equations. As expected, these similar resulting stresses show that the FE model is in reasonable agreement with plate theory. A discussion regarding the equivalence of the predicted in-plane stress and the modeled von Mises equivalent stress is found in Appendix B.

The model resulted in deflections of 24.05 μm at each of the outside edges compared to a deflection of 23.74 μm at the center of the cantilever. This model result suggests that an inadvertent deflection measurement taken along the edge of the cantilever would give a deflection, and subsequent stress prediction, 1.3% higher than a measurement taken along the cantilever's midline. This source of potential error is reasonably low, especially when considering that the deflected cantilever stress measurement technique is typically used for qualitative comparison purposes. Figure 5 shows differences in deflection along the width (i.e. short axis) of the cantilever.

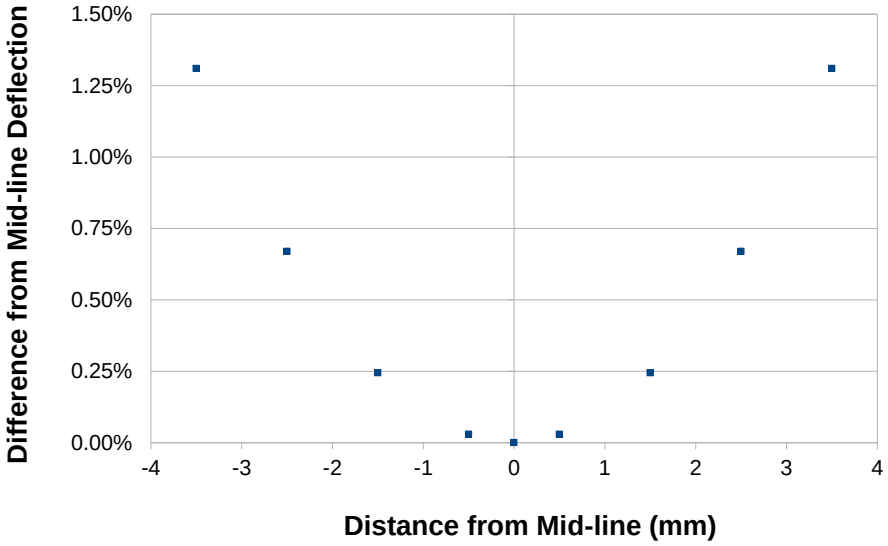

Figure 5: Differences in deflection along the width (i.e. short axis) of the cantilever. Deflections are shown as percent difference from the deflection at the cantilever's mid-line.

3 Potential Effect on Stress Prediction from Border used to Eliminate Lateral Drying Fronts: Soft Caulk Border Analysis

3.1 Background

One issue typical of the deflected beam measurement method is the presence of a drying front that begins at the edges of the cantilever and progresses toward the center until the entire coating has dried. Such fronts create gradients in the coating stress which invalidate the plate theory relationships. As a result, deflection measurements cannot be used to determine the stress during the drying process of these samples. It was discovered through the work of Karan Jindal [2] that the

application of a soft caulk material as a border around the edges of the cantilever eliminates this lateral drying front and allows the coating to dry uniformly. The border eliminates the lateral drying front by altering the interface at the edge of the cantilever and allowing the liquid coating to retain a constant thickness leading to this edge – as opposed to thinning near the edge and promoting a faster drying time than experienced at the center of the cantilever. FE analysis was used in order to understand the decreased deflection, and subsequent measurement error, due to the additional stiffness and reduced coating area caused by the caulk border.

3.2 Finite Element Model

The model was intended to simulate a coating of alumina particles dispersed in water spread inside a caulk border over a silicon cantilever. This analysis was performed by comparing three similar but distinct models using ANSYS version 11.0 software. The first model simulated a fully coated cantilever with no border. The second model simulated a coated cantilever with a border – coating was absent where the border overlapped onto the cantilever. The third model simulated a coated cantilever without a border, but also with coating absent where the border would have overlapped onto the cantilever. The purpose of this third model was to understand the portion of total error created by the additional stiffness of the border material as opposed to the loss in deflection created by the absence of coating in the border overlap region. Each of the three models is illustrated in Figure 10.

Cantilever, coating, and border material geometries of the simulated sample are listed below. The border dimensions represent more caulk material than would

normally be present and serve as a worst-case condition with respect to measurement error.

- Cantilever
    - Length = 45 mm
    - Width = 8 mm
    - Thickness = 0.400 mm (400 μm)
- Coating Thickness = 0.010 mm (10 μm)
- Caulk Border Cross-section = 2 mm x 2 mm (not including overlap region)
- Caulk Border Overlap
    - 0.100 mm (100 μm) along each long edge
    - 0.200 mm (200 μm) along each short edge

In order to reduce model size and solution time, symmetry about the long axis of the cantilever was used so only half of the cantilever required modeling. A constraint was placed on the bisected faces of the cantilever, coating, and border such that rotation about the long axis was zero (i.e. rotation about the X-axis equals zero – reference Figure 9 and Figure 10). This constraint allowed for appropriate bending along the short axis of the cantilever (i.e. cupping) without the presence of the opposite half of the sample.

All adjacent volumes representing the cantilever, the coating, and the border material were joined using the "glue" Boolean operation within ANSYS. A three-

dimensional, 20 node structural solid named “Solid95” was chosen as the element type (see Figure 2).

Experiments were conducted to measure the mechanical properties of the caulk border material. Compressive modulus of the caulk was found to be approximately 4.5 MPa. Tensile modulus was found to be approximately 2 MPa (two experiments were conducted with results of 2.2 MPa and 1.6 MPa). A conservative modulus of 5 MPa was assigned to the border material in the finite element models. Stress strain plots for compression and tensile testing of the caulk are shown in Figure 6, Figure 7, and Figure 8.

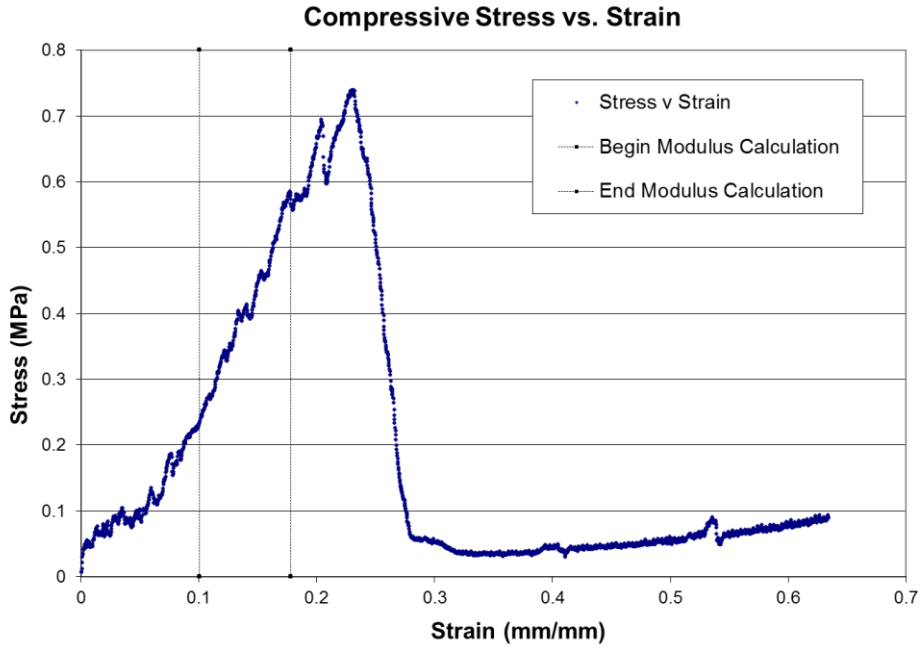

Figure 6: Compressive Stress vs. Strain (Compressive Modulus = 4.5 MPa)

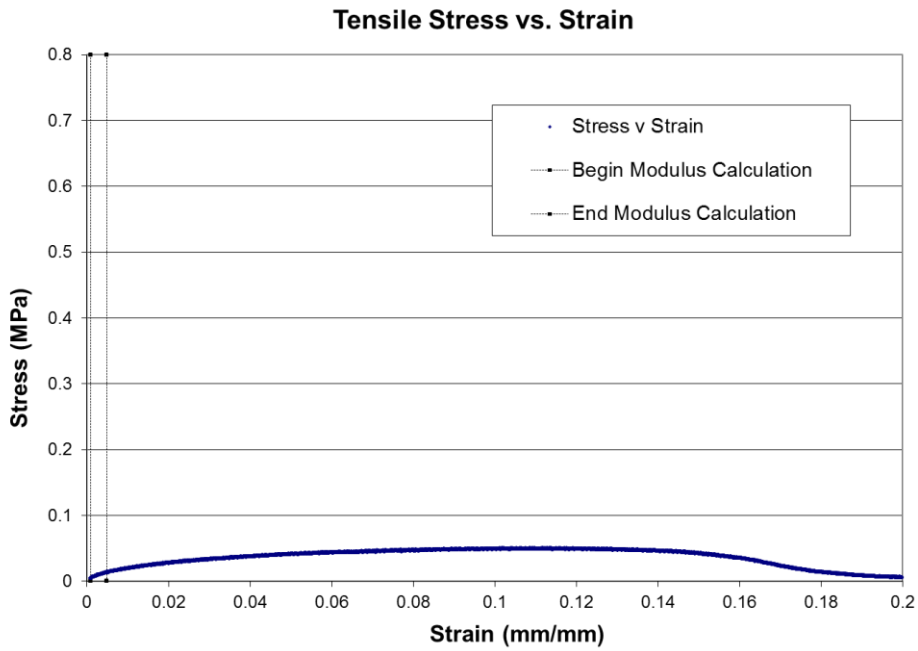

Figure 7: Tensile Stress vs. Strain (run #1, Tensile Modulus = 2.2 MPa)

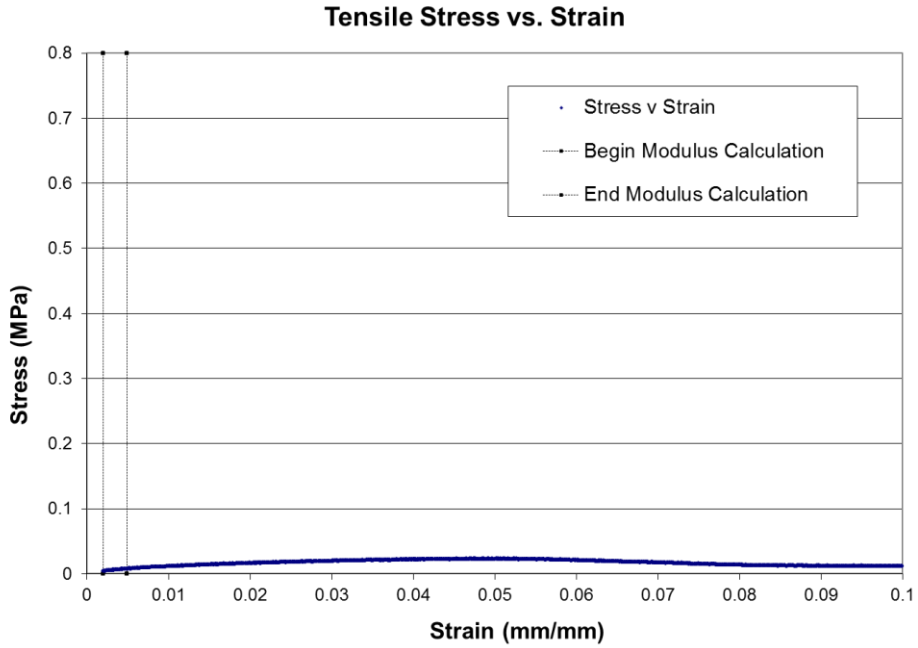

Figure 8: Tensile Stress vs. Strain (run #2, Tensile Modulus = 1.6 MPa)

Material properties used in the FE model are listed below:

- $E_{cantilever}$ = 172 GPa
- $\nu_{cantilever}$ = 0.25
- $E_{coating}$ = 3 GPa
- $\nu_{coating}$ = 0.33
- $E_{caulk\ border}$ = 5 MPa
- $\nu_{caulk\ border}$ = 0.33

A hexahedral mesh was created by dividing the cantilever and caulk border into elements of size 0.10 mm x 0.10 mm x 0.10 mm (length x width x height) and the coating into elements of size 0.10 mm x 0.10 mm x 0.01 mm. The meshed volumes of the coated cantilever with caulk border model are shown in Figure 9.

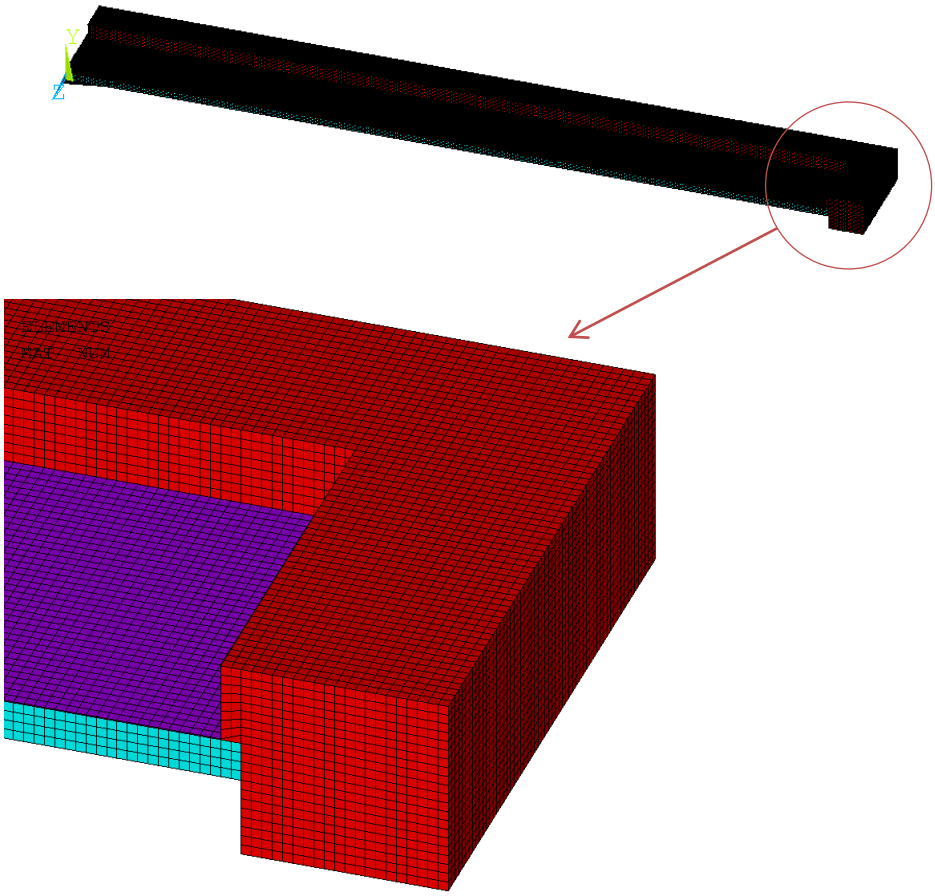

Figure 9: Meshed Volumes of Coated Cantilever with Caulk Border Model

Drying of the coating and its associated constrained shrinkage were simulated within the FE model by applying a thermal contraction to the coating. All coating elements were given a coefficient of thermal expansion of 0.001 [1/degree]. A temperature load of -2 degrees was applied to the coating resulting in a constrained shrinkage of 0.2%. In order to replicate clamping of the sample into the test apparatus, the cantilever and border or coating (whichever would be adjacent to the

clamp) were constrained by setting all degrees of freedom for all areas at X = 0 to zero.

3.3 Results and Discussion

As expected, the solution plots, given in Figure 10, show each of the cantilevers deflecting smoothly upward.

(a)

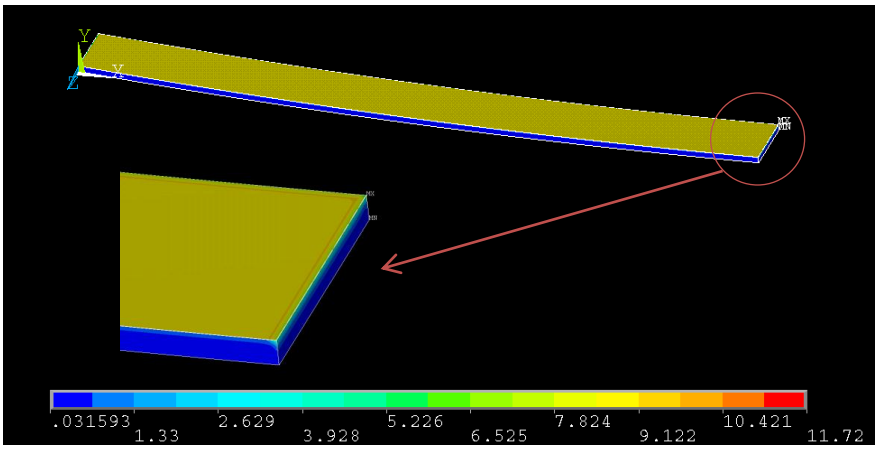

(b)

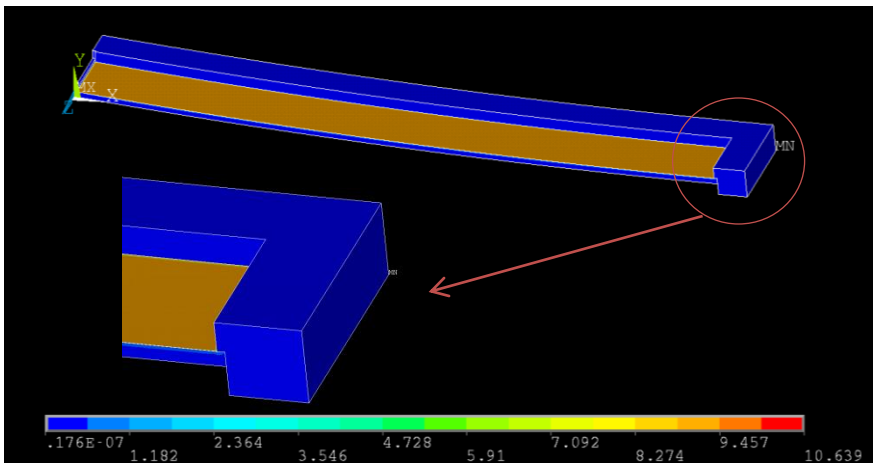

(c)

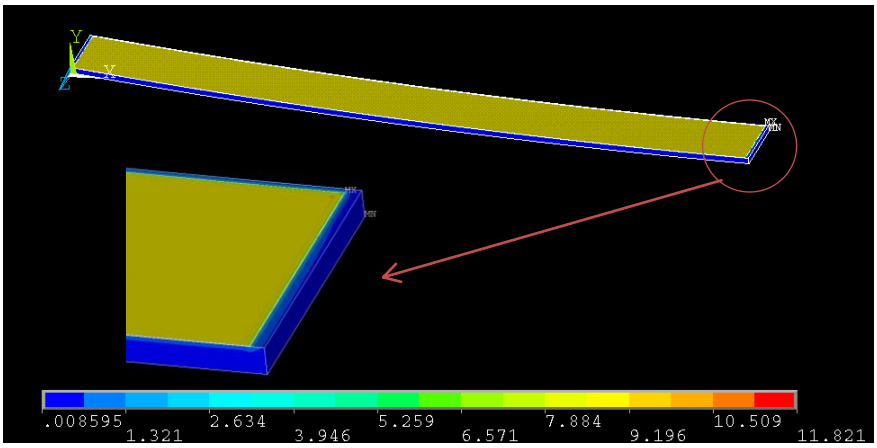

Figure 10: von Mises Equivalent Stress Plots of the Deformed Cantilevers: (a) fully coated with no border, (b) coated cantilever with border, and (c) coated cantilever without border and coating absent where border would be present

Deflections for each of the modeled cantilevers were taken from a point on the under-side of the cantilever along its center line (Z = 0 mm) at 30 mm from its clamped/constrained end (X = 30 mm). This simulates a typical measurement location targeted by the laser used to detect the deflection of lab samples.

Deflections of the three modeled cantilevers at this point were similar but slightly different from each other. As would be expected the sample with complete coating and no border resulted in the highest deflection. The smallest deflection was found for the sample which included the border. The deflection of the sample with no border but with coating absent in the areas of border overlap was between those of the other two models. Deflection results for each of these samples are given in Table 1.

Table 1: Cantilever Deflection Results for Caulk Border Analysis

Model Description	Modeled Deflection	
	Resulting Model Cantilever Deflection (μm)	**Difference from Fully Coated Model**
Fully Coated Cantilever 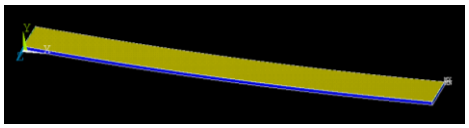	7.0174	N/A
Caulk Border is Present – Coating Absent at Overlap 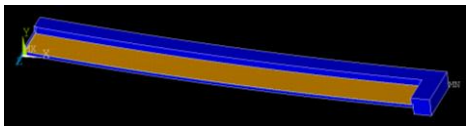	6.7202	-4.24%
Caulk Border is not Present – Coating Absent at Overlap 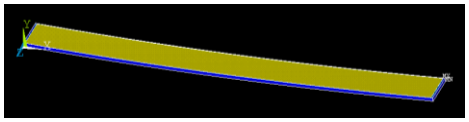	6.7322	-4.06%

Figure 10 above shows consistent coating stress (indicated by lack of color gradient) over each cantilever. Modeled von Mises equivalent coating stress was taken at three locations in each of the models: 30 mm from its clamped/constrained end (X = 30) at 1 mm, 2 mm, and 3 mm from the cantilever's center line (Z = -1 mm, -2 mm, and -3 mm). The resulting local coating stress was very similar in each of the three models. This is intuitive as each of the three models subjects the coating to the same 0.2% constrained shrinkage. Modeled von Mises equivalent coating stresses are compiled in Table 2.

Table 2: Modeled von Mises Coating Stress for the Caulk Border Analysis

Model Description	Modeled Coating Stress	
	Resulting Model Coating Stress (MPa)	**Difference from Fully Coated Model**
Fully Coated Cantilever 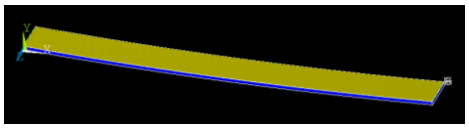	8.9368	N/A
Caulk Border is Present – Coating Absent at Overlap 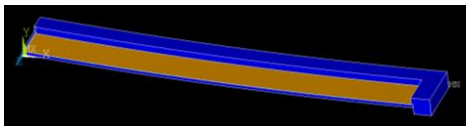	8.9370	0.002%
Caulk Border is not Present – Coating Absent at Overlap 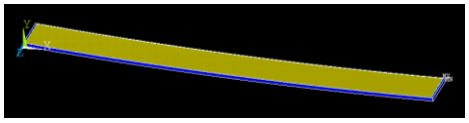	8.9370	0.002%

* Note: Resulting coating stress was taken at three points and each point gave the same stress value.

The primary goal of this analysis was to understand the error introduced to a coating stress prediction as a result of using a caulk border. Table 3 gives the stress predictions calculated by applying the in-plane stress equations to the deflections listed in Table 1. The differences in calculated stress from the "ideal" fully coated cantilever model are also given for the other two models.

Table 3: Calculated Average Coating Stresses using Modeled Deflection Results

Model Description	In-plane Stress Calculated from Modeled Deflection	
	Calculated In-plane Average Stress (MPa)	**Difference from Fully Coated Model**
Fully Coated Cantilever 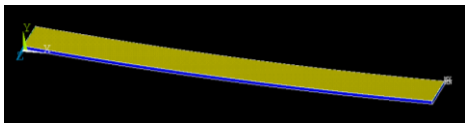	9.304	N/A
Caulk Border is Present – Coating Absent at Overlap 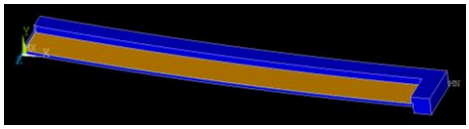	8.910	-4.24%
Caulk Border is not Present – Coating Absent at Overlap 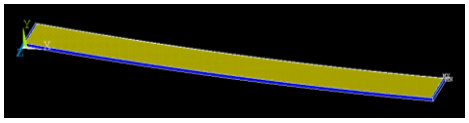	8.926	-4.06%

The model which included the caulk border resulted in a predicted stress 4.24% lower than that of the fully coated model. This level of error is reasonably low, especially when considering that the deflected cantilever stress measurement technique is typically used for qualitative comparison purposes.

The model without the border but with coating absent in the area of border overlap gave a predicted stress which was similar to that of the model which included the border (-4.06% difference from the fully coated model vs. -4.24% difference from the fully coated model). This result indicates that most of the error introduced by the border is due to a reduction in coated area caused by the border's overlap onto the

cantilever. This assertion is supported by the observation that despite having deflection differences of approximately 4%, the local coating stresses found in each of the three models were nearly identical.

4 Potential Effect on Stress Prediction from Border used to Eliminate Lateral Drying Fronts: Photoresist Border Analysis

4.1 Background

A second border material, photoresist deposited in layers onto a silicon cantilever, is being explored by Kathleen Crawford at the University of Minnesota as another option to eliminate lateral drying. The photoresist border also eliminates the lateral drying front by altering the interface at the edge of the cantilever and allowing the liquid coating to retain a constant thickness leading to this edge – as opposed to thinning near the edge and promoting a shorter drying time than experienced at the center of the cantilever. An FE analysis, similar to that of the caulk border described above, was used to understand the decreased deflection, and subsequent measurement error, due to the additional stiffness and reduced coating area caused by photoresist border.

4.2 Finite Element Model

The model was intended to simulate a latex coating inside a photoresist border over a silicon cantilever. This analysis was performed by comparing three similar but distinct models using ANSYS version 11.0 software. The first model simulated a fully coated cantilever with no border. The second model simulated a coated

cantilever with a border – coating was absent where the border overlapped onto the cantilever. The third model simulated a coated cantilever without a border, but also with coating absent where the border would overlap onto the cantilever if it were present. The purpose of this third model was to understand the portion of total error created by the additional stiffness of the border material as opposed to the loss in deflection created by the absence of coating in the border overlap region. Each of the three models is illustrated in Figure 12.

Cantilever, coating, and border material geometries of the simulated sample are listed below.

- Cantilever
    - Length = 45 mm
    - Width = 6 mm
    - Thickness = 0.500 mm (500 μm)
- Coating Thickness = 0.075 mm (75 μm)
- Photoresist Border
    - Width = 0.050 mm (50 μm)
    - Thickness/Height = 0.200 mm (200 μm)

In order to reduce model size and solution time, symmetry about the long axis of the cantilever was used so only half of the cantilever required modeling. A constraint was placed on the bisected faces of the cantilever, coating, and border such that rotation about the long axis was zero (i.e. rotation about the X-axis equals zero –

reference Figure 11 and Figure 12). This constraint allowed for appropriate bending along the short axis of the cantilever (i.e. cupping) without the presence of the opposite half of the sample.

All adjacent volumes representing the cantilever, the coating, and the border material were joined using the "glue" Boolean operation within ANSYS. A three-dimensional, 20 node structural solid named "Solid95" was chosen as the element type (see Figure 2).

Modulus of the photoresist border, SU-8 2000 (MicroChem, Newton, MA), was taken from a technical data sheet provided by the manufacturer. The coating was modeled as latex. Material properties used in the FE model are listed below:

- $E_{cantilever}$ = 172 GPa
- $\nu_{cantilever}$ = 0.25
- $E_{coating}$ = 3 GPa
- $\nu_{coating}$ = 0.33
- $E_{photoresist\ border}$ = 2 GPa
- $\nu_{photoresist\ border}$ = 0.30

The first model, simulating the fully coated cantilever, used a hexahedral mesh which divided the cantilever into elements of size 0.100 mm x 0.100 mm x 0.100 mm (length x width x height) and the coating into elements of size 0.100 mm x 0.100 mm x 0.075 mm. The remaining two models, simulating the presence of the border and/or absence of coating in the overlap region, used a hexahedral mesh which divided the

cantilever and border into elements of size 0.050 mm x 0.050 mm x 0.050 mm (length x width x height) and the coating into elements of size 0.050 mm x 0.050 mm x 0.0375 mm. The additional resolution was needed for the latter two models due to the small width (50 µm) of the photoresist border. The meshed volumes of the coated cantilever with photoresist border model are shown in Figure 11.

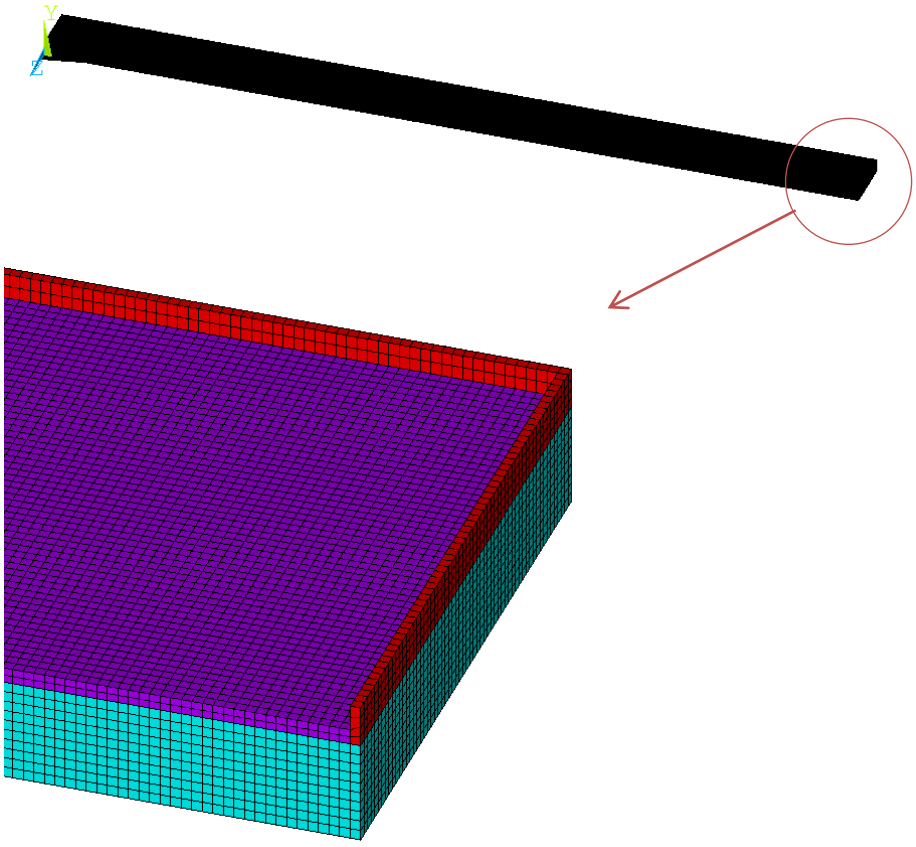

Figure 11: Meshed Volumes of Coated Cantilever with Photoresist Border Model

Drying of the coating and its associated constrained shrinkage was simulated within the FE model by applying a thermal contraction to the coating. All coating

elements were given a coefficient of thermal expansion of 0.001 [1/degree]. A temperature load of -2 degrees was applied to the coating resulting in a constrained shrinkage of 0.2%. In order to replicate clamping of the sample into the test apparatus, the cantilever and border or coating (whichever was adjacent to the clamp) were constrained by setting all degrees of freedom for all areas at X = 0 to zero.

4.3 Discussion and Results

As expected, the solution plots, given in Figure 12, show each of the cantilevers deflecting smoothly upward.

(a)

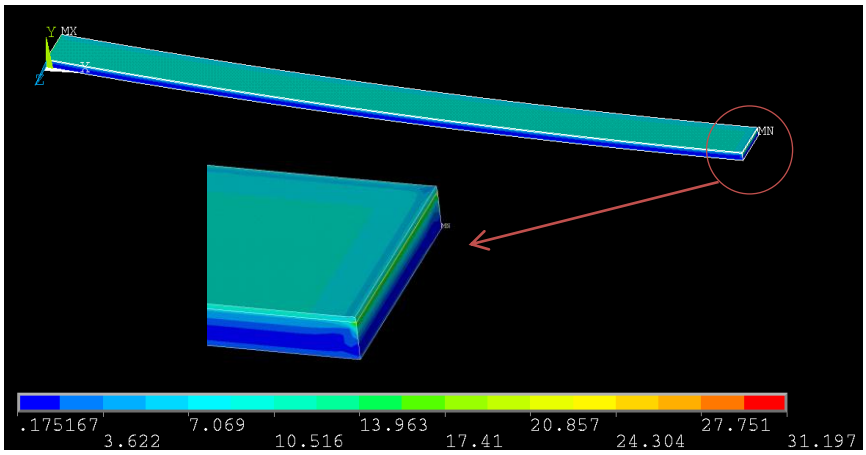

(b)

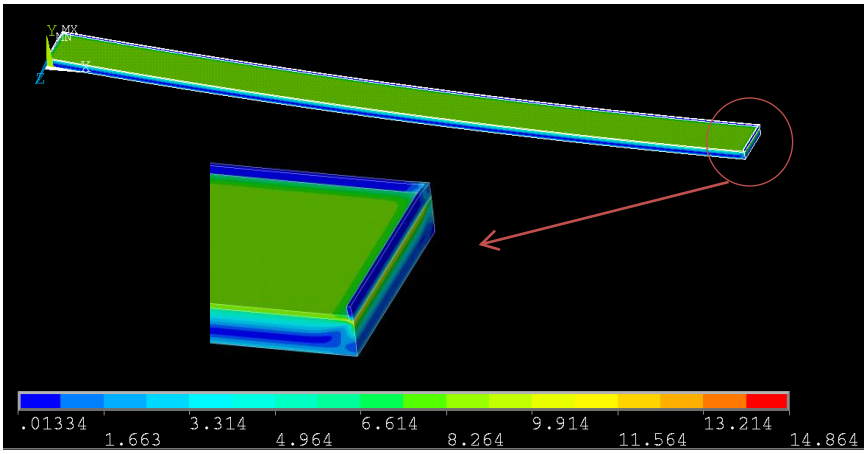

(c)

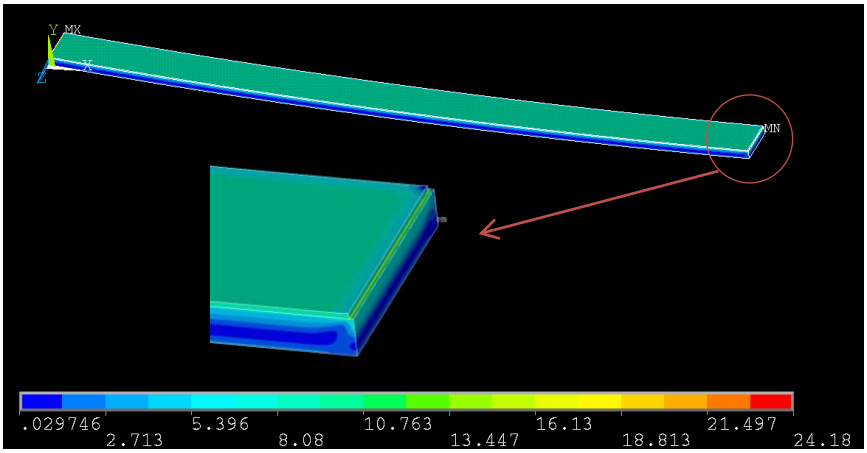

Figure 12: von Mises Equivalent Stress Plots of the Deformed Cantilevers: (a) fully coated with no border, (b) coated cantilever with border, and (c) coated cantilever without border and coating absent where border would be present

Deflections for each of the modeled cantilevers were taken from a point on the under-side of the cantilever along its center line (Z = 0 mm) at 30 mm from its clamped/constrained end (X = 30 mm). This simulates a typical measurement location targeted by the laser used to detect the deflection of lab samples.

Deflections of the three modeled cantilevers at this point were similar to but slightly different from each other. As would be expected the sample with complete coating and no border resulted in the highest deflection. The smallest deflection was found for the sample which included the border. The deflection of the sample with no border but with coating absent in the areas of border overlap was between those of the other two models. Deflection results for each of these samples are compiled in Table 4.

Table 4: Cantilever Deflection Results for the Photoresist Border Analysis

Model Description	Modeled Deflection	
	Resulting Model Cantilever Deflection (μm)	**Difference from Fully Coated Model**
Fully Coated Cantilever 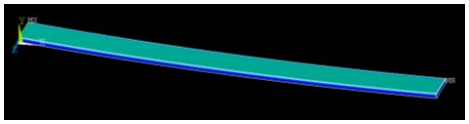	36.925	N/A
Photoresist Border is Present – Coating Absent at Overlap 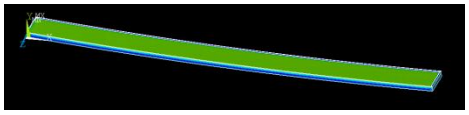	35.917	-2.73%
Photoresist Border is not Present – Coating Absent at Overlap 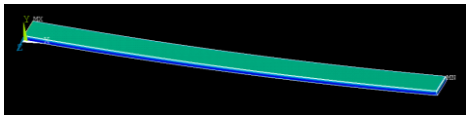	36.307	-1.67%

Figure 12 above shows consistent coating stress (indicated by lack of color gradient) over each cantilever. Modeled von Mises equivalent coating stress was taken at three locations in each of the models: 30 mm from its clamped/constrained end (X = 30) at 0.5 mm, 1.5 mm, and 2.5 mm from the cantilever's center line (Z = -0.5 mm, -1.5 mm, and -2.5 mm). The resulting local coating stress was very similar in each of the three models. This is intuitive as each of the three models subjects the coating to the same 0.2% constrained shrinkage. Each of the three models showed coating stress to be slightly different at 2.5 mm from the center of the cantilever as this was only 0.5 mm from the edge of the cantilever and 0.45 mm from the edge of the border. Modeled von Mises equivalent coating stresses are compiled in Table 5.

Table 5: Modeled von Mises Equivalent Coating Stress for the Photoresist Border Analysis

Model Description	Modeled Coating Stress	
	Resulting Model Coating Stress (MPa)	**Difference from Fully Coated Model**
Fully Coated Cantilever 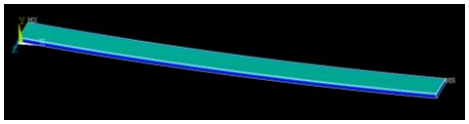	0.5 mm: 8.8136 1.5 mm: 8.8136 2.5 mm: 8.7887	
	Mean = 8.8053	N/A
Photoresist Border is Present – Coating Absent at Overlap 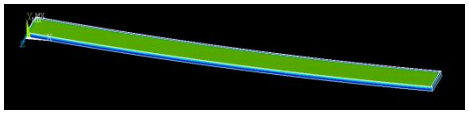	0.5 mm: 8.8145 1.5 mm: 8.8145 2.5 mm: 8.7783	
	Mean = 8.8024	-0.033%
Photoresist Border is not Present – Coating Absent at Overlap 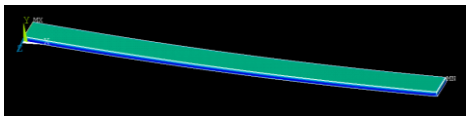	0.5 mm: 8.8145 1.5 mm: 8.8145 2.5 mm: 8.7705	
	Mean = 8.7998	-0.062%

The primary goal of this analysis was to understand the error introduced to a coating stress prediction as a result of using the photoresist border. Table 6 gives the stress predictions calculated by applying the in-plane stress equations to the deflections listed in Table 4. The differences in calculated stress from the "ideal" fully coated cantilever model are also given for the other two models.

Table 6: Calculated Average Coating Stresses using Modeled Deflection Results

Model Description	In-plane Stress Calculated from Modeled Deflection	
	Calculated In-plane Average Stress (MPa)	**Difference from Fully Coated Model**
Fully Coated Cantilever 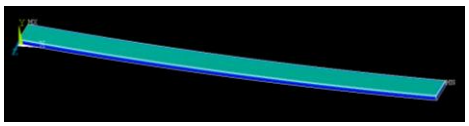	9.091	N/A
Photoresist Border is Present – Coating Absent at Overlap 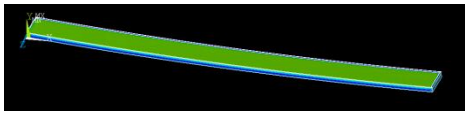	8.843	-2.73%
Photoresist Border is not Present – Coating Absent at Overlap 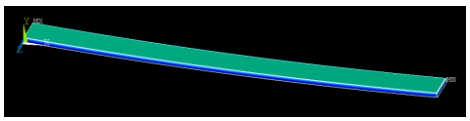	8.939	-1.67%

The model which included the photoresist border resulted in a predicted stress 2.73% lower than that of the fully coated model. This level of error is reasonably low, especially when considering that the deflected cantilever stress measurement technique is typically used for qualitative comparison purposes.

The model without the border but with coating absent in the area of border overlap resulted in a predicted stress 1.67% lower than that of the fully coated model. This result indicates that the largest portion of error introduced by the photoresist border is due to a reduction in coated area caused by the border's overlap onto the

cantilever. The remaining, slightly smaller, portion of error may be assigned to the additional stiffness provided by the photoresist border.

5 Analysis of Coating Stress over a Cantilever throughout Lateral Drying and Relaxation

5.1 Finite Element Model

Finite element analysis was used to explore the relationship between cantilever deflection, coating stress, dried area, and relaxed area under the presence of a lateral drying front. Lateral drying conditions were modeled by dividing the coating into 32 sections of equal width (16 on each side of the central axis), and then simulating the progressive drying of each section starting at the outside of the cantilever and ending with its inner-most section. After each section had simulated drying, an analogous relaxation process was modeled by allowing each section to relax – again one section per time step from the outside of the cantilever to its center.

The analysis was intended to simulate a coating of ceramic particles (typically alumina or silica) dispersed in water with a polymer binder (typically polyvinyl alcohol) over a silicon cantilever and was performed using ANSYS version 11.0 software. A cantilever, similar to those simulated in analyses above, was modeled to a length of 45 mm and a width of 8 mm. The coating, however, was modeled as 16 individual 0.25 mm strips in order to facilitate progressive drying and relaxation toward and from the center of the sample (respectively). Cantilever and coating geometries of the simulated sample are listed below.

- Cantilever Length = 45 mm
- Cantilever Width = 8 mm
- Cantilever Thickness = 0.400 mm (400 μm)
- Coating Thickness = 0.010 mm (10 μm)

In order to reduce model size and solution time, symmetry about the long axis of the cantilever was used so only half of the cantilever required modeling. A constraint was placed on the bisected faces of the cantilever and coating such that rotation about the long axis was zero (reference Figure 13). This constraint allowed for appropriate bending along the short axis of the cantilever (i.e. cupping) without the presence of the opposite half of the sample.

All adjacent volumes representing the cantilever and the coating were joined using the "glue" Boolean operation within ANSYS. A three-dimensional, 20 node structural solid named "Solid95" was chosen as the element type (see Figure 2).

Material properties of the cantilever and coating used in the FE model are listed below:

- $E_{cantilever}$ = 172 GPa
- $\nu_{cantilever}$ = 0.25
- $E_{coating}$ = 3 GPa
- $\nu_{coating}$ = 0.33

A hexahedral mesh was created by dividing the cantilever into elements of size 0.100 mm x 0.100 mm x 0.100 mm (length x width x height) and the coating into elements of size 0.100 mm x 0.083 mm x 0.010 mm.

All coating elements were given a coefficient of thermal expansion of 0.001 [1/degree]. During the drying phase of the analysis (steps 1 – 16), each successive strip was "dried" by applying a thermal load of -2 degrees. This resulted in a constrained shrinkage of 0.2% simulating the behavior of a dried coating. The coating strips were dried from the outside edge of the cantilever to the center of the cantilever in order to emulate the lateral drying front.

During the relaxation phase of the analysis (steps 17 – 32), each successive strip of coating was 'relaxed' by replacing the initial thermal load of -2 degrees with a relaxed thermal load of -1 degree. This caused the strip to relax to a constrained shrinkage of 0.1%. The strips were relaxed from the outside edge of the cantilever to the center of the cantilever.

The solution plots illustrated in Figure 13 show each of the cantilevers deflecting smoothly upward. Deflection increases progressively through completion of the drying phase (step 16). Deflection subsequently decreases from its peak value during the relaxation phase and continues to decrease until relaxation is complete. Figure 13 shows von Mises equivalent stress plots of the coated cantilever models after steps 2, 8, 16, 18, 24, and 32.

(a)

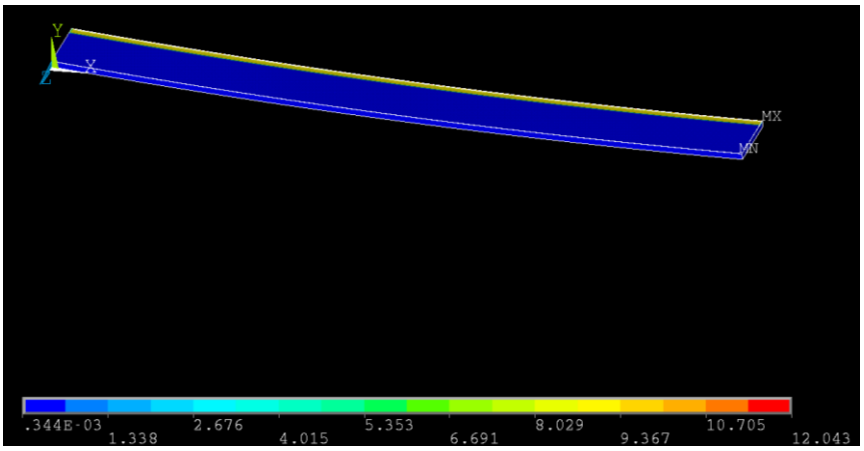
Y
Z
X
MX
MN
.344E-03
1.338
2.676
4.015
5.353
6.691
8.029
9.367
10.705
12.043

(b)

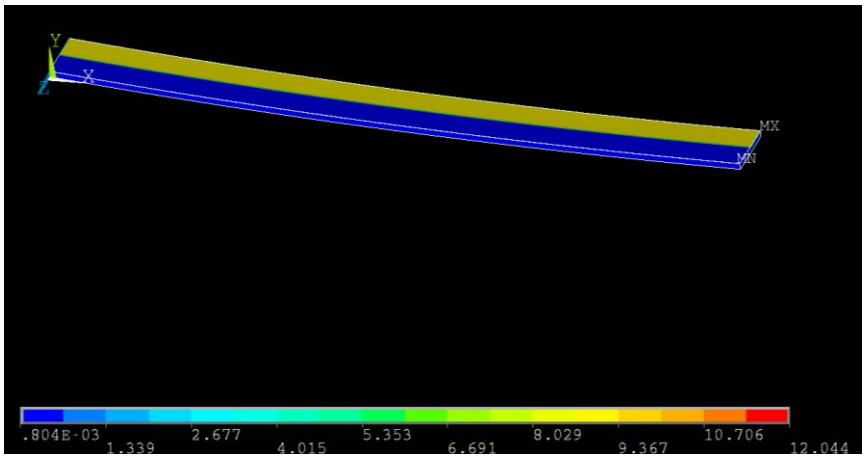
Y
Z
X
MX
MN
.804E-03
1.339
2.677
4.015
5.353
6.691
8.029
9.367
10.706
12.044

(c)

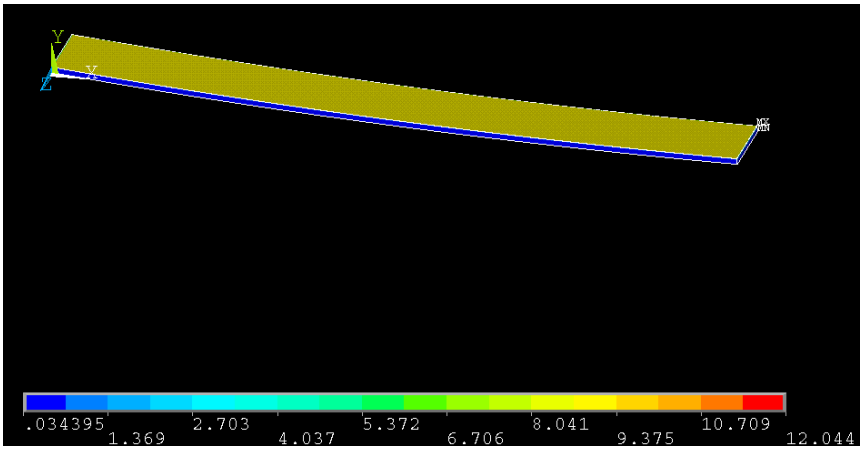
Y
Z
X
MX
MN
.034395
1.369
2.703
4.037
5.372
6.706
8.041
9.375
10.709
12.044

(d)

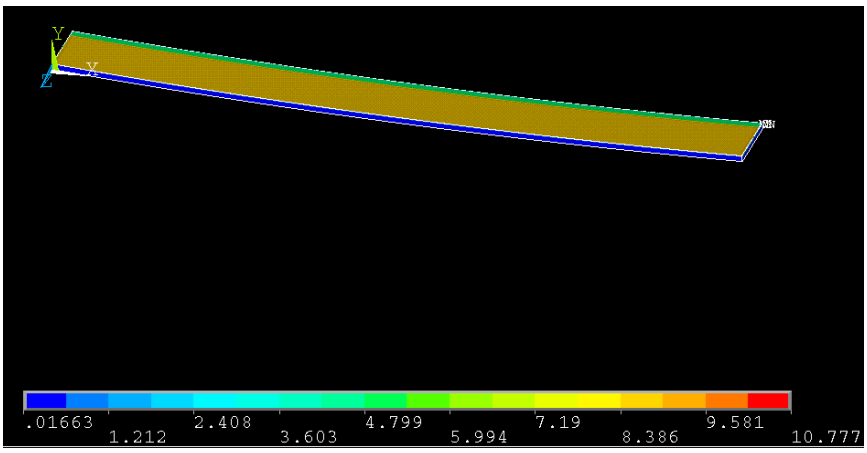

(e)

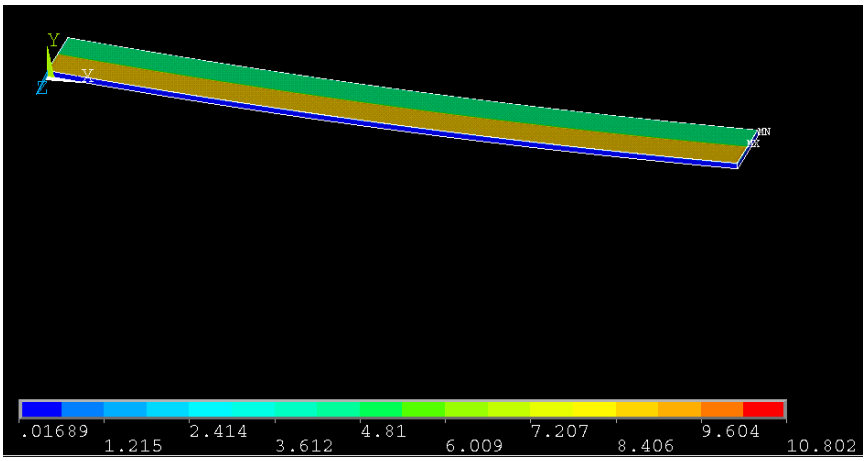

(f)

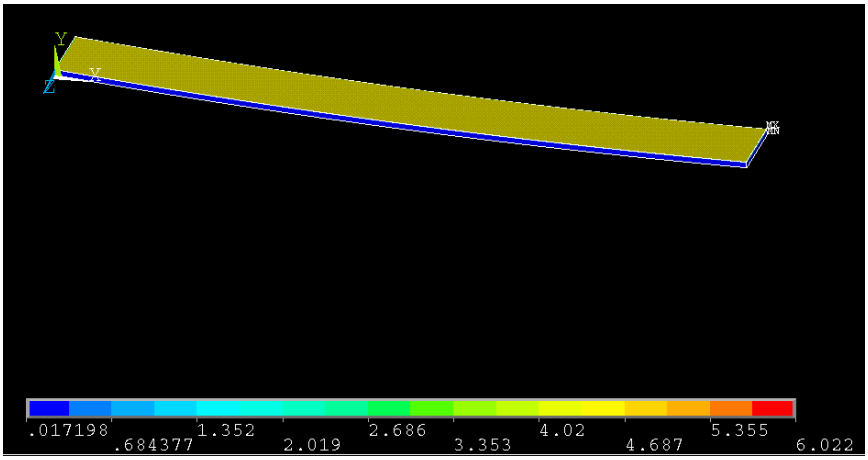

Figure 13: von Mises Equivalent Stress Plot of the Coated Cantilever after selected steps in the drying process: (a) after step 2, (b) after step 8, (c) after step 16, (d) after step 18, (e) after step 24, (f) after step 32.

5.2 Relationship between Deflection and Dried / Relaxed Coating Fraction

Table 7 gives the modeled cantilever deflection results for each of the drying and relaxation steps. Table 7 also gives an estimated cantilever deflection for each of the drying and relaxation steps – this estimation is calculated using the dried coating fraction (or relaxed coating fraction) multiplied by the deflection at the end of the drying (or relaxation) phase. The error between the modeled deflection and the estimated deflection is approximately 5% when the drying front is near the edge of the cantilever and decreases as the drying front advances toward the center.

Table 7: Modeled Deflection, Estimated Deflection, and Resulting Error

Time Step	Process	Fraction	Modeled Deflection (μm)	Deflection Estimated from Dried / Relaxed Fraction (μm)	Error
1	Drying	0.0625	0.4170	0.4386	5.17%
2	Drying	0.1250	0.8396	0.8772	4.47%
3	Drying	0.1875	1.2667	1.3157	3.87%
4	Drying	0.2500	1.6980	1.7543	3.32%
5	Drying	0.3125	2.1328	2.1929	2.82%
6	Drying	0.3750	2.5706	2.6315	2.37%
7	Drying	0.4375	3.0109	3.0700	1.96%
8	Drying	0.5000	3.4531	3.5086	1.61%
9	Drying	0.5625	3.8970	3.9472	1.29%
10	Drying	0.6250	4.3421	4.3858	1.01%
11	Drying	0.6875	4.7879	4.8243	0.76%
12	Drying	0.7500	5.2342	5.2629	0.55%
13	Drying	0.8125	5.6807	5.7015	0.37%
14	Drying	0.8750	6.1269	6.1401	0.21%
15	Drying	0.9375	6.5725	6.5786	0.09%
16	Drying	1.0000	7.0172	7.0172	0.00%

17	Relaxing	0.0625	6.8087	6.7979	-0.16%
18	Relaxing	0.1250	6.5974	6.5786	-0.28%
19	Relaxing	0.1875	6.3839	6.3593	-0.38%
20	Relaxing	0.2500	6.1682	6.1401	-0.46%
21	Relaxing	0.3125	5.9508	5.9208	-0.50%
22	Relaxing	0.3750	5.7319	5.7015	-0.53%
23	Relaxing	0.4375	5.5118	5.4822	-0.54%
24	Relaxing	0.5000	5.2907	5.2629	-0.53%
25	Relaxing	0.5625	5.0687	5.0436	-0.49%
26	Relaxing	0.6250	4.8462	4.8243	-0.45%
27	Relaxing	0.6875	4.6233	4.6050	-0.40%
28	Relaxing	0.7500	4.4001	4.3858	-0.33%
29	Relaxing	0.8125	4.1769	4.1665	-0.25%
30	Relaxing	0.8750	3.9538	3.9472	-0.17%
31	Relaxing	0.9375	3.7310	3.7279	-0.08%
32	Relaxing	1.0000	3.5086	3.5086	0.00%

The relationship between the modeled and estimated deflections is plotted in Figure 14. It can be seen that deflection increases nearly proportionally with the fraction of area behind the drying front as stress increases. In a similar manner, deflection decreases nearly proportionally with the fraction of area behind the relaxation front as stress decreases. This is interesting as it suggests that each strip contributes a similar amount to the cantilever's deflection regardless of its location.

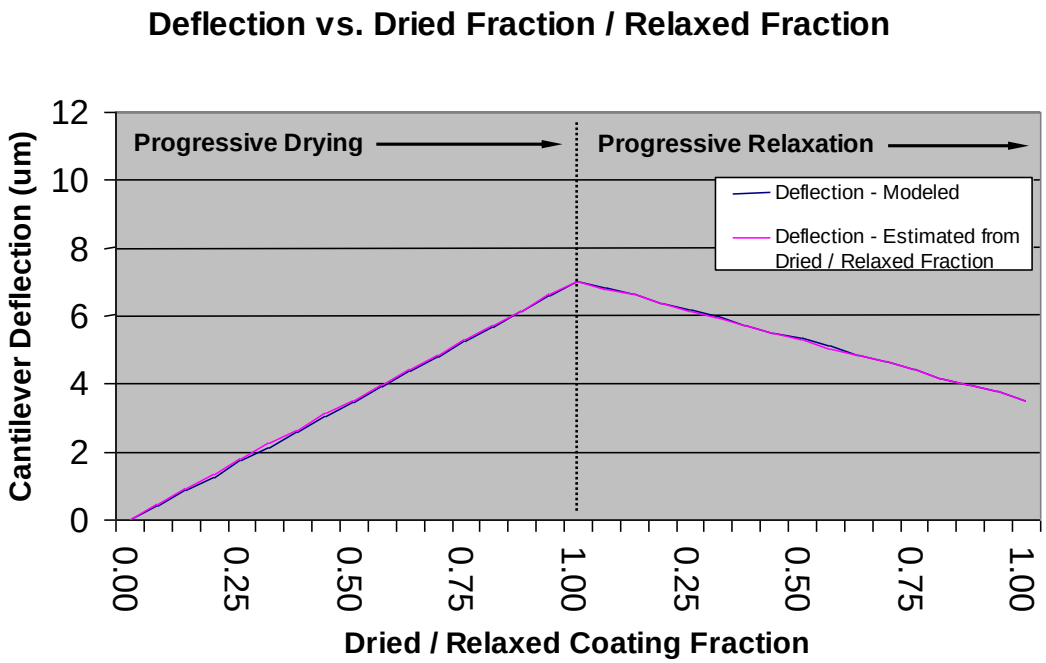

Figure 14: Modeled Deflection and Estimated Deflection vs. Dried Fraction and Relaxed Fraction

5.3 Relationship between Coating Stress and Dried / Relaxed Coating Fraction

The lateral drying front progresses inward as each successive strip of coating dries. As it dries, each strip reaches its peak stress and sustains a stress level near this peak until relaxation begins. The von Mises equivalent stress present in each strip of coating is represented by the thin lines of Figure 15. The first line increasing to its peak stress represents the outermost strip of coating, the second line increasing to its peak stress represents the next strip inward, and so on.

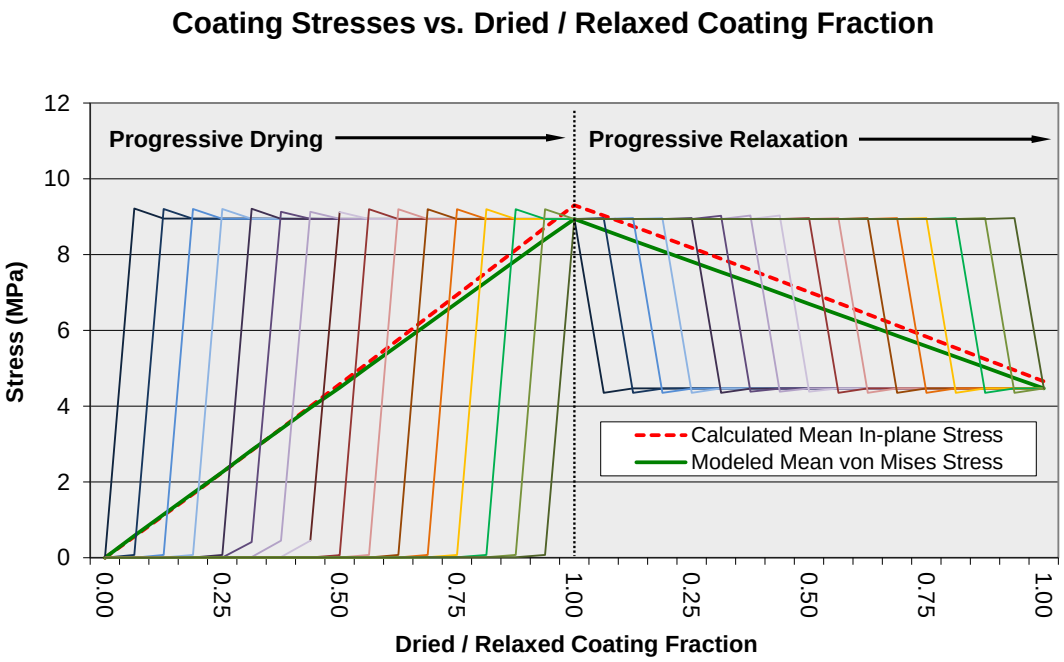

Figure 15: Modeled Mean von Mises Equivalent Stress and Calculated Mean In-plane Stress vs. Dried Fraction and Relaxed Coating Fraction

Mean coating stress over the width of the cantilever can be calculated by summing the von Mises equivalent stress present in each coating strip normalized for its width fraction. This mean coating stress may be expressed as

$$\sigma_{mean} = \sum \sigma_i \frac{w_i}{W} \qquad (1)$$

where,

σ_i = stress present in individual coating strip

w_i = width of individual coating strip

W = width of cantilever

For example, the mean coating stress averaged across the entire cantilever resulting from two 0.25 mm strips (one on either side of the cantilever) experiencing an 8 MPa stress would be 0.5 MPa when taken over the cantilever's width of 8 mm.

The mean coating stress calculated using the modeled stress for each strip of coating and Equation 1 is represented in Figure 15 by the solid green line. In a similar manner to the cantilever's deflection discussed in section 5.2 above, the mean coating stress also increases and decreases linearly as the coating dries and relaxes.

Generally, the in-plane stress equation developed from plate theory and shown as Equation 2 (also Equation A-18 in Appendix A) is used to calculate average in-plane stress of a coating as it dries uniformly over a cantilever (i.e. not exhibiting lateral drying behavior). However, despite the intentional presence of lateral drying, when the FE model's cantilever deflection results are applied to Equation 2 the resulting stress profile is very similar to that generated using the mean coating stress of Equation 1.

$$S = \frac{dEt^3}{3cl^2(t+c)(1-\nu)} \qquad (2)$$

where,

$S =$ mean in-plane coating stress

d = deflection of cantilever

E = modulus of substrate

t = thickness of substrate

c = thickness of coating

l = length along plate where deflection is measured

v = Poisson's ratio of substrate

Average in-plane stress per Equation 2 is shown in Figure 15 as the dashed red line. It trends closely with mean coating stress generated by Equation 1 giving a maximum error of approximately 5% (see Table 8 for tabulated results including error values). This close relationship will be used in the sections below as a means to estimate local coating stresses based on deflection observations of a coated cantilever sample despite the presence of lateral drying. A discussion regarding the equivalence of the average in-plane stress predicted from plate theory relationships and the modeled von Mises equivalent stress is found in Appendix B.

Table 8: Comparison between Modeled Mean Stresses and Calculated Mean Stresses

Time Step	Process	Fraction	Modeled Mean von Mises Stress (MPa)	Calculated Mean In-plane Stress (MPa)	Error
1	Drying	0.0625	0.581	0.553	-4.90%
2	Drying	0.1250	1.140	1.113	-2.37%
3	Drying	0.1875	1.700	1.679	-1.18%
4	Drying	0.2500	2.259	2.251	-0.33%
5	Drying	0.3125	2.841	2.828	-0.45%
6	Drying	0.3750	3.397	3.408	0.33%
7	Drying	0.4375	3.955	3.992	0.94%

8	Drying	0.5000	4.489	4.578	1.99%
9	Drying	0.5625	5.052	5.167	2.27%
10	Drying	0.6250	5.611	5.757	2.61%
11	Drying	0.6875	6.169	6.348	2.91%
12	Drying	0.7500	6.727	6.940	3.17%
13	Drying	0.8125	7.285	7.532	3.39%
14	Drying	0.8750	7.842	8.123	3.59%
15	Drying	0.9375	8.400	8.714	3.74%
16	Drying	1.0000	8.937	9.304	4.10%
17	Relaxing	0.0625	8.652	9.027	4.34%
18	Relaxing	0.1250	8.373	8.747	4.47%
19	Relaxing	0.1875	8.093	8.464	4.58%
20	Relaxing	0.2500	7.814	8.178	4.66%
21	Relaxing	0.3125	7.539	7.890	4.66%
22	Relaxing	0.3750	7.262	7.600	4.65%
23	Relaxing	0.4375	6.982	7.308	4.66%
24	Relaxing	0.5000	6.699	7.015	4.71%
25	Relaxing	0.5625	6.418	6.720	4.72%
26	Relaxing	0.6250	6.138	6.425	4.67%
27	Relaxing	0.6875	5.859	6.130	4.62%
28	Relaxing	0.7500	5.580	5.834	4.55%
29	Relaxing	0.8125	5.301	5.538	4.48%
30	Relaxing	0.8750	5.021	5.242	4.40%
31	Relaxing	0.9375	4.742	4.947	4.31%
32	Relaxing	1.0000	4.469	4.652	4.10%

5.4 Estimating Stress behind a Drying Front from Experimental Observations

A close relationship exists between the mean coating stress calculated as the normalized sum of the individual coating strips (per Equation 1) and the mean in-plane coating stress calculated using observed cantilever deflection along with equations derived from plate theory (per Equation 2). This close relationship suggests that

experimentally observed deflection measurements may be used to estimate coating stresses behind a lateral drying front as follows.

1. Measure the deflection of a cantilever subject to a lateral drying front.
2. Use Equation 2 to calculate the mean in-plane stress along the width of the cantilever.
3. Assign all stress to the portion of the coating behind the drying front. This may be accomplished by dividing the overall mean stress by the fraction of the coating which is behind the drying front as

$$\sigma_{local} = \frac{\sigma_{mean}}{\chi_{dried}} \qquad (3)$$

Note: The relationship in Equation 3 assumes relaxation is not yet present in the dried portion of the coating.

6 Potential Method for Deducing Local Stress vs. Time Profile from Mean Coating Stress vs. Time Profile

6.1 Motivation

The analysis and relationships developed in the previous section suggest that the Stress vs. Time profile of a coated cantilever progressing through the drying process can be estimated as the sum of the local Stress vs. Time profiles. Inversely, it may also be possible to deduce the stress evolution profile of a small (local) region of coating by examining the stress evolution profile and drying behavior of a complete

coated cantilever sample. Such a method would be very useful if it allowed for the construction of the local stress evolution profile despite the presence of lateral drying.

6.2 Description of a Potential Technique for Constructing a Local Stress Profile

Figure 16 illustrates a theoretical local Stress vs. Time profile for a small (local) region of coating. Certain attributes of this profile are labeled within the figure. These attributes along with necessary experimental observations are described in Table 9. The intent is that this information may be observed from a coated cantilever sample displaying lateral drying behavior and then used to estimate the local coating stress profile. Figure 17 illustrates the necessary attributes as they might appear on the theoretical Stress vs. Time profile of a lateral drying coated cantilever sample.

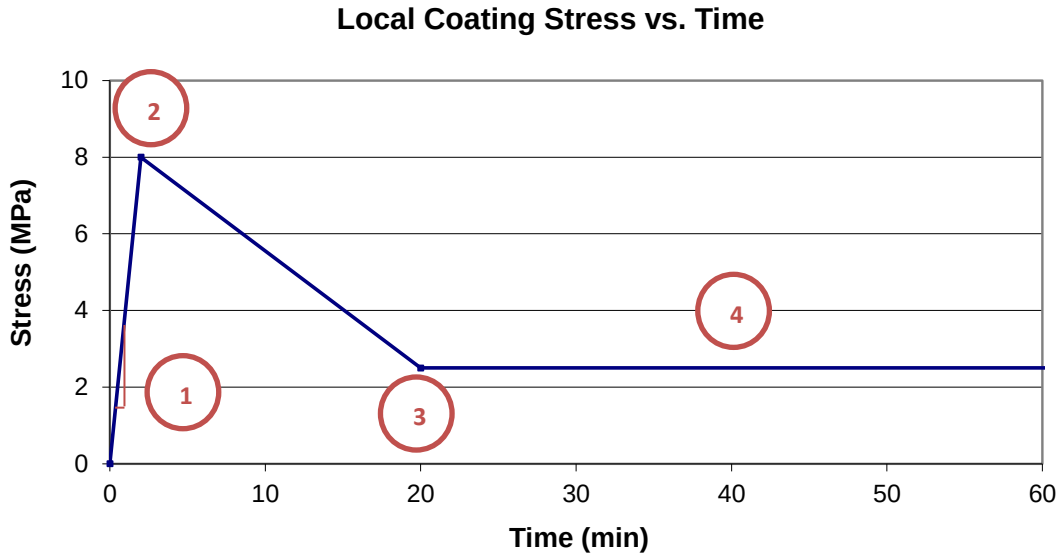

Figure 16: Theoretical Average In-plane Stress vs. Time for Small Local Region of Coating

Table 9: Attributes used to Build Theoretical Local Coating Stress vs. Time Profile

Identifier	Attribute Description	Example Value from Profiles
1	**Initial Rate of Local Stress Increase** This is the initial slope of the Local Coating Stress vs. Time profile. Identifying the Attribute: This is calculated as the initial slope of the Average In-plane Coating Stress profile (Figure 17) normalized to reflect the dried coating fraction (analogous to Equation 3).	4 MPa / min
2	**Time to Initiation of Local Stress Relaxation** This is the time at which the Local Coating Stress vs. Time profile peaks and relaxation begins. Identifying the Attribute: This is the time at which the initial slope of the Average In-plane Coating Stress profile (Figure 17) begins to decrease.	2 min
3 and Observation from Video Recording	**Time to Completion of Local Stress Relaxation** This is the time required from initiation of local drying until local stress relaxation is completed. Identifying the Attribute: This is the difference in time between the completion of drying over the full cantilever (observed from video recording) and complete relaxation of the full cantilever (observed from Figure 17).	35 min - 15 min 20 min
4	**Relaxed Stress** This is the local stress after stress relaxation has been completed. Identifying the Attribute: This is the steady-state Average In-plane Coating Stress (from Figure 17) after stress relaxation has been completed.	2.5 MPa
N/A – Observation from Video	**Drying Rate** Note: Drying rate would only be used to	0.25 mm / min

Recording	recreate a fully coated cantilever stress profile for the purposes of validating the local stress profile (see discussion below). Drying rate defines the time offset between the initiation of each subsequent local stress evolution profile (i.e. when the drying front reaches a particular location). The summation of individual local stresses at each time point estimates the Average In-plane Coating Stress over the cantilever. Identifying the Attribute: This is the rate at which the lateral drying front advances through the coating as observed in a video recording of the sample as it dries.	

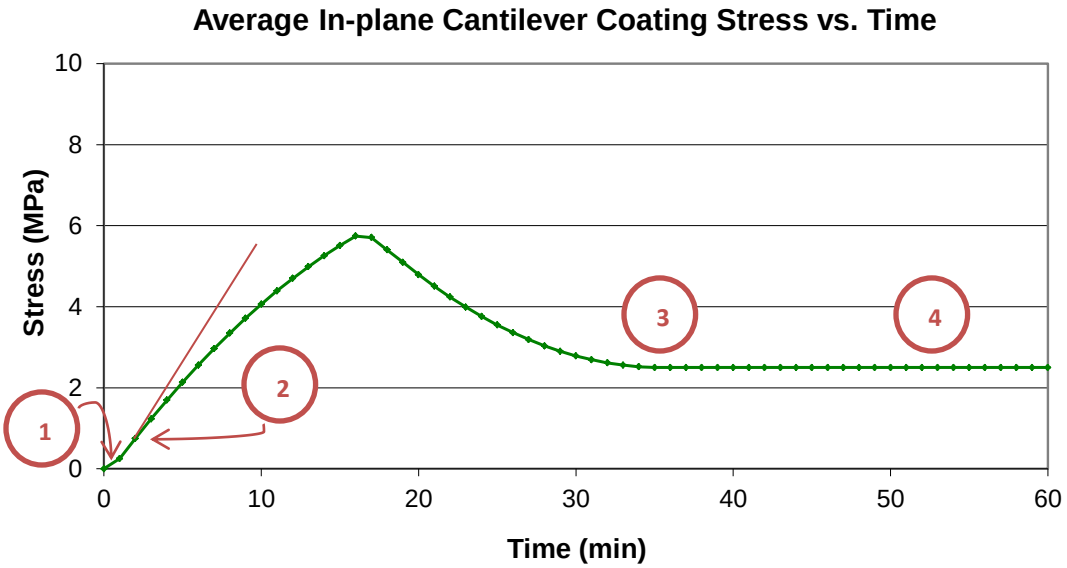

Figure 17: Theoretical Average In-plane Coating Stress vs. Time for Coated Cantilever

6.3 Approach to Validating Potential Technique for Constructing a Local Stress Profile

The resulting local stress evolution profile obtained from the technique described in section 6.2 could be validated by using it to recreate the stress evolution profile of the full coated cantilever sample. Approximating a full sample profile could be achieved by summing the stresses experienced by each local coating region (each normalized for its area fraction) at each point in time. The time at which each local stress profile is initiated (i.e. stress begins to rise) is deduced by observing, with the aid of a video recorder, the speed at which the lateral drying front proceeds through the coated cantilever sample. The accuracy of the local stress evolution profile would be supported if the recreated full sample stress evolution profile successfully approximated the experimentally observed full sample stress evolution profile.

Use of this technique could be further supported by creating a sample very similar to the lateral drying sample discussed above (same cantilever material and dimensions, same coating and thickness, etc.) with the exception that the lateral drying front is eliminated. This could be achieved using a border around the cantilever as discussed in sections 3 and 4. An average in-plane stress evolution profile of the non-lateral drying sample which closely approximated the local coating stress evolution profile, deduced from a lateral drying experiment, would further support the local stress profile construction technique.

7 Challenges in Constructing a Local Stress Evolution Profile from Experimental Data

The execution of the approach described in section 6 for estimating the local stress evolution profile can be challenging. The drying of each coated cantilever lab sample is unique and its stress profile will contain noise and possibly unanticipated features. The stress profile of a coated cantilever lab sample and its associated drying rate data are shown in Figure 18. This sample consisted of a silica–polyvinyl alcohol (PVA) coating (43 wt% PVA) over a silicon cantilever. The sample was prepared in a manner similar to that described by Jindal [2]. No border was used and the sample displayed lateral drying behavior. The sample was allowed to dry in ambient temperature and relative humidity conditions – nitrogen cover gas was not used. The average final thickness of the coating was 8.75 μm.

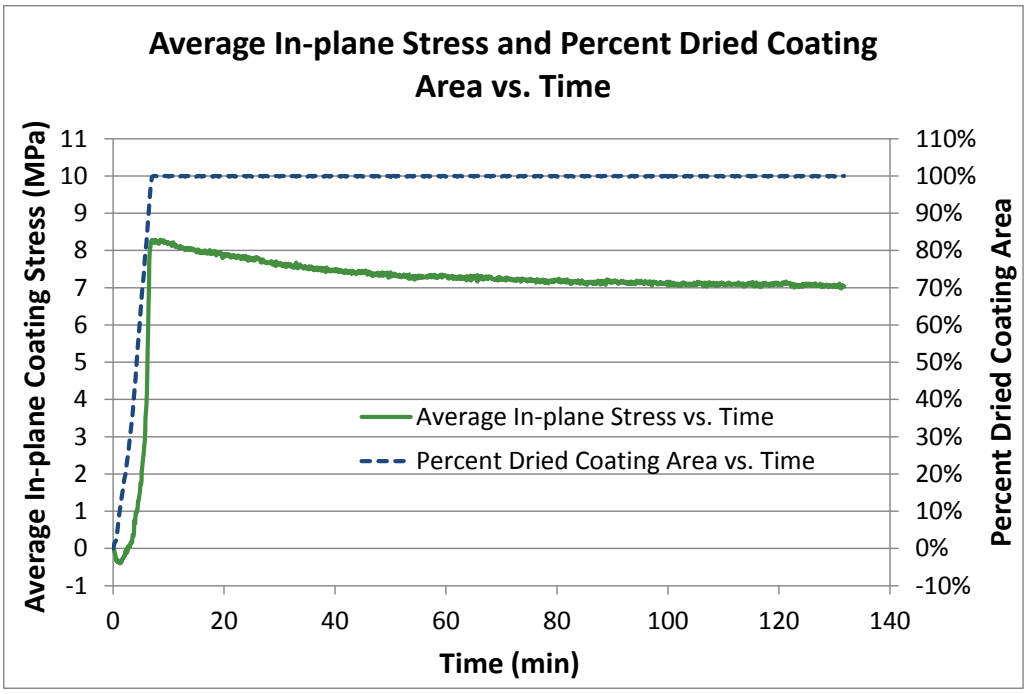

Figure 18: Calculated Average In-plane Coating Stress and Percent Dried Coating Area vs. Time for Coated Cantilever Lab Sample

Data obtained during the experiment, illustrated in Figure 18, allowed for estimation of two of the necessary attributes described in section 6.2. The video recording showed complete drying of the coating at approximately 7 minutes. Figure 18 shows complete relaxation at approximately 120 minutes, although it is difficult to precisely mark this event due to the very slow decay of coating stress as well as the subtle noise inherent to the measurement technique. Therefore, the time to completion of local stress relaxation (attribute #3) can be estimated at 113 minutes (120 minutes – 7 minutes). Additionally, the relaxed coating stress (attribute #4) is approximately 7.0 MPa.

Unfortunately, the remaining two attributes necessary to construct a local stress profile could not be obtained from this data set. The Stress vs. Time profile above includes a decrease just after Time = 0 which brings stress to a negative value. It is not known exactly what caused this dip into negative stress, but similar behavior has been observed by other experimenters [3]. Regardless of the cause, this profile does not allow for (i) the initial rate of local stress increase or (ii) the time to initiation of local stress relaxation (attributes #1 and #2 discussed in section 6.2). As a result, this particular data set does not allow for an estimation of the local coating stress profile.

Another potential source of error in estimating local stress evolution could be variation in coating thickness. Measurements taken after drying was complete showed that the average coating thickness near the midline of the sample was 10.5 μm while the average coating thickness between the midline and each edge was 7.9 μm.

8 Future Work

Additional experiments, similar to that described above, could be performed in an effort to deduce a local stress evolution profile from the observations of a coated cantilever sample under lateral drying conditions. Experimental technique may need to be refined in order to eliminate the initial stress reduction. Additional refinement may be necessary to sufficiently estimate the initial slope of the Stress vs. Time curve as well as to locate the time at which this slope begins to decrease (i.e. identification of attributes #1 and #2).

If these refinements were to be made, a successful deduction of the local stress profile may be possible. The summation of these local profiles, accounting for an initial delay at each local position consistent with the observed drying rate data, should reasonably approximate the experimentally observed Stress vs. Time profile of the full cantilever sample.

Further comparison of the constructed local stress profiles could be made against stress profiles of uniform drying samples (i.e. non-lateral drying samples) achieved with the use of a border along the cantilever's edges. Similar stress evolution profiles for the constructed local stress and the uniform drying samples would indicate that both methods (local stress construction and border-induced uniform drying) successfully estimate the local coating stress.

References

[1] E. M. Corcoran; *Journal of Paint Technology*; 41(538), 635 – 640 (1969).

[2] K. Jindal; Stress Development in Particulate, Nano-composite and Polymeric Coatings, Ph.D Thesis; University of Minnesota (2009).

[3] C. Petersen, C. Heldmann, and D. Johannsmann; *Langmuir*, Vol. 15, No. 22, 7745 – 7751 (1999).

Appendix A: Development of In-plane Stress Equations

Background and Assumptions

The purpose of the following derivation is to develop a relationship in which coating stress can be calculated by measuring deflection of a cantilever on which the coating dries and applying this deflection to the known properties of the cantilever substrate along with the coating's thickness. This relationship was originally developed by Corcoran [1] and is commonly used to calculate the average in-plane stress within a uniform coating as it dries. The "in-plane" stress refers to the stress parallel to the plane of the cantilever. Stress perpendicular to the plane of the cantilever is assumed to be zero as the coating is not constrained in this direction (i.e. it is free to become thinner during the drying process).

It should be noted that this derivation relies on plate theory, which accounts for the bi-directional coating stress, as opposed to beam theory which accounts for stress in only one direction (e.g. in the "long" direction of the cantilever). Due to the long, thin shape of the plate used for coating experiments, the term "cantilever" will be used at certain points throughout this discussion to describe the plate. The assumptions below also apply to the derivation.

- Curvature of plate is spherical
- Strain is less than 3 – 5% at all locations in the plate
- The elastic limit of plate is not exceeded
- The plate is either vertical or is stiff enough / light enough that the effects of gravity are negligible

- The elastic properties of the coating and substrate are isotropic
- The coating adheres to the substrate
- Shrinkage differences and stress variation around edges (and at different points through thickness) are negligible

Development of Derivation

A thin plate will be bent to a spherical curvature if the bending moments along the edges are equal.

If $m_x = m_y = m$, the curvature of the plate is given by

$$\frac{1}{r_x} = \frac{1}{r_y} = \frac{1}{r} = \frac{m}{D(1+\nu)} \qquad \text{(A-1)}$$

where D is the flexural rigidity of the plate,

$$D = \frac{Et^3}{12(1-\nu^2)} \qquad \text{(A-2)}$$

and

r = radius of curvature of the bent plate

m = bending moment per unit length

υ = Poisson's ratio of the plate

E = elastic modulus of the plate

t = plate thickness

Combining Equations A-1 and A-2 gives:

$$\frac{1}{r} = \frac{12m(1-\nu)}{Et^3} \qquad \text{(A-3)}$$

Assuming the beam is fixed at one end, the deflection is related to the radius of curvature as illustrated in Figure 19 and described in Equation A-4:

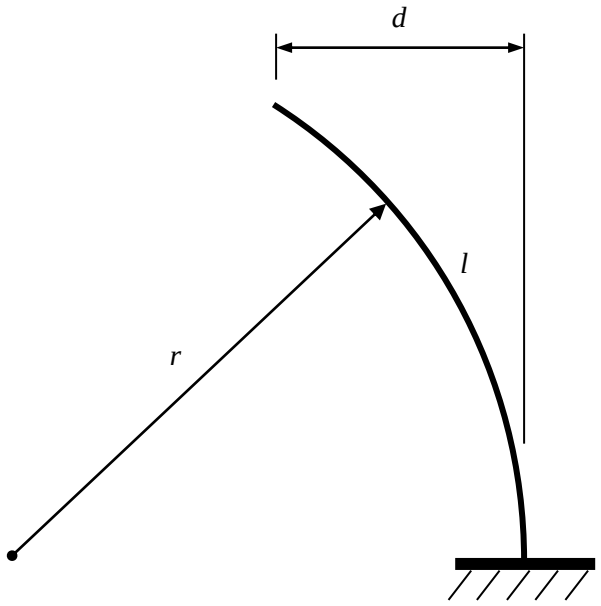

Figure 19: Illustration of a Beam with Length *l* Deflected a Distance *d* and to a Radius of Curvature *r*

$$\frac{1}{r} = \frac{2d}{l^2} \quad \text{(A-4)}$$

d = deflection

l = length of plate

Combining Equations A-3 and A-4 gives:

$$d = \frac{6ml^2(1-\nu)}{Et^3} \quad \text{(A-5)}$$

The beam bends due to the compressive force in the coating and its resultant force is imparted through the coating-plate interface. However, this force can also be expressed as a moment which results in the same radius of curvature.

This moment can be expressed as

$$M_w = \frac{F_w(t+c)}{2} \quad \text{(A-6)}$$

as illustrated by Figure 20 which shows the system at equilibrium:

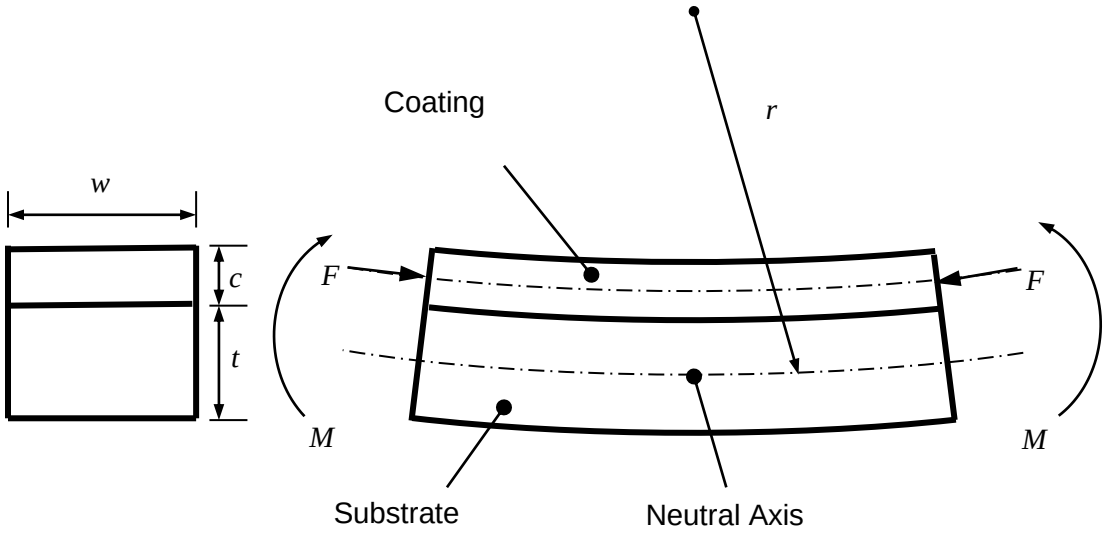

Figure 20: Illustration of the equivalent moments applied to a beam resulting from compressive stresses within the coating

where M is the total moment applied to each end, and

$$F = S_{eq} A_c = S_{eq} wc \qquad \text{(A-7)}$$

$$M_w = \frac{S_{eq} wc(t+c)}{2} \qquad \text{(A-8)}$$

S_{eq} = average force applied half-way into the coating thickness

w = width of coating

Equations A-1, A-3, and A-5 defined m as the bending moment per unit length. Therefore, Mw and m are related by the following expression:

$$\frac{M_w}{w} = m \tag{A-9}$$

Combining Equations A-8 and A-9 gives:

$$m = \frac{M_w}{w} = \frac{S_{eq}c(t+c)}{2} \tag{A-10}$$

Combining Equations A-5 and A-10 gives:

$$d = \left(\frac{6l^2(1-\nu)}{Et^3}\right)\left(\frac{S_{eq}c(t+c)}{2}\right) \tag{A-11}$$

$$S_{eq} = \frac{dEt^3}{3cl^2(t+c)(1-\nu)} \tag{A-12}$$

Equation A-12 reflects the average in-plane stress found in the coating when the cantilever is in the bent position. Most practical substrates used for production applications, however, would not bend nearly as readily as the cantilever used for experimental purposes.

If the in-plane stress of the same coating applied to a completely rigid surface is of interest, the difference in strain can be added as follows:

$$S = S_{eq} + \varepsilon_{cd} E_c \qquad \text{(A-13)}$$

Where

E_c = Elastic modulus of the coating

The strain term, ε_{cd}, must also include the perpendicular component:

$$\varepsilon_{cd} = \frac{S_{(f-f')}}{E_c} - \frac{\nu_c S_{\perp}(f-f')}{E_c} \qquad \text{(A-14)}$$

where

υ_c = Poisson's ratio of the coating

Because the coating is assumed isotropic, Equation A-14 simplifies to the following:

$$\varepsilon_{cd} = \frac{S_{(f-f')}(1-\nu_c)}{E_c} \qquad \text{(A-15)}$$

It can be shown that

$$\varepsilon_{cd} = \frac{(\frac{t+c}{2})}{r} \tag{A-16}$$

Substituting r as expressed in equation A-4 into equation A-16 and combining with Equations A-12, A-13, and A-15 yields the following:

$$S = \frac{dEt^3}{3cl^2(t+c)(1-\nu)} + \frac{dE_c(t+c)}{l^2(1-\nu_c)} \tag{A-17}$$

However, because the elastic modulus of the cantilever is at least two orders of magnitude greater than that of the coating and is also at least one order of magnitude thicker, the second term of Equation A-17 can be eliminated without introducing significant error (< 1%). This allows the average in-plane stress equation to be simplified to the following:

$$S = \frac{dEt^3}{3cl^2(t+c)(1-\nu)} \tag{A-18}$$

The relationship described by Equation A-18 can be used to calculate the average in-plane stress in a coating. Assuming the cantilever's elastic modulus,

Poisson's ratio, thickness, and location of its deflection measurement are known, the only measurements needed to calculate the in-plane coating stress are the deflection of the cantilever and the thickness of the coating.

Appendix B: Relationship between Experimentally Calculated In-plane Stress and Modeled von Mises Equivalent Stress in the Coating

The analyses in this report routinely compare the von Mises equivalent stress of a coating obtained from FE models to the in-plane coating stress (i.e. coating stress in the plane parallel to the cantilever substrate) calculated through plate theory relationships (see Appendix A). The discussion below explains why the von Mises equivalent stress and the in-plane stress are equivalent for the scenario of the coated cantilever explored throughout this report.

Consider an infinitesimally small region of coating, its position over the cantilever, and the orientation of its principal stresses as illustrated in Figure 21.

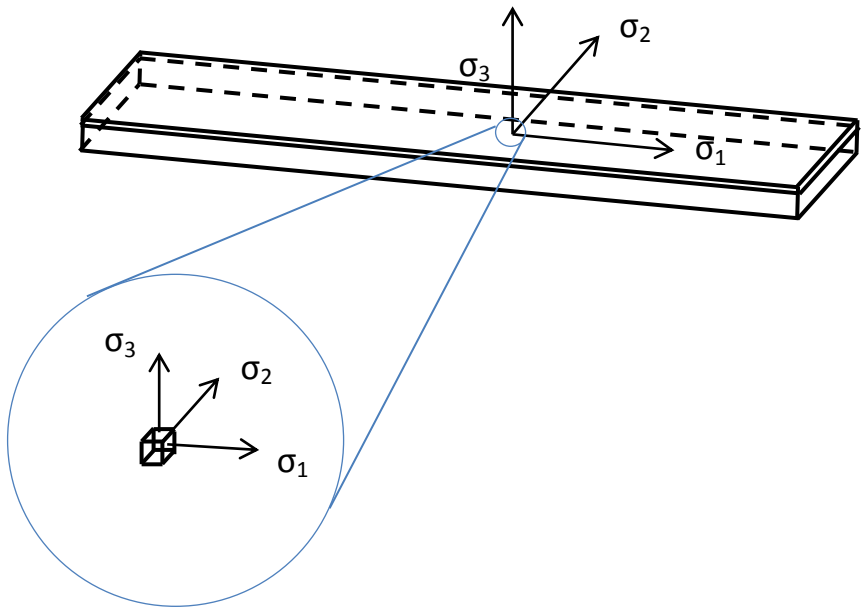

Figure 21: Illustration of an infinitesimally small region of coating over a cantilever

The von Mises equivalent stress which identifies the maximum stress created by a given set of principal stresses may be expressed by the following:

$$\sigma_{eq} = \sqrt{\frac{(\sigma_1-\sigma_2)^2+(\sigma_2-\sigma_3)^2+(\sigma_1-\sigma_3)^2}{2}} \qquad \text{(B-1)}$$

Because the coating material is isotropic and constrained shrinkage is the same in every direction within the plane over the cantilever, the stresses experienced by the infinitesimally small region in each direction within the plane (i.e. the "in-plane" stress) have the same magnitude. Additionally, because shrinkage is not constrained through the thickness of the coating, no stress is experienced in the direction perpendicular to the cantilever's surface. It should be noted that both of these behaviors are consistent with results from the FE models. These relationships can be expressed as follows:

$$\sigma_1 = \sigma_2 = \sigma_{In-Plane} \qquad \text{(B-2)}$$

$$\sigma_3 = 0 \qquad \text{(B-3)}$$

Application of Equations B-2 and B-3 into Equation B-1 simplifies as follows:

$$\sigma_{eq} = \sqrt{\frac{(\sigma_1-\sigma_2)^2+(\sigma_2-\sigma_3)^2+(\sigma_1-\sigma_3)^2}{2}} = \sqrt{\frac{{\sigma_1}^2+{\sigma_2}^2}{2}} = \sqrt{\frac{2\sigma_{1,2}^2}{2}} = \sigma_{1,2}$$

$$\therefore \quad \sigma_{eq} = \sigma_{1,2} = \sigma_{In-Plane} \qquad \text{(B-4)}$$

This relationship shows that the von Mises equivalent stress correctly identifies the maximum stress as the in-plane stress. This is the same in-plane stress which is calculated experimentally through the use of measured deflection and plate theory relationships.